NASA TECHNICAL NOTE

NASA TN D-8131

NASA TN D-8131

EFFECTS OF FOUR INLET AND OUTLET TIP-ANNULUS-AREA BLOCKAGE CONFIGURATIONS ON THE PERFORMANCE OF AN AXIAL-FLOW FAN ROTOR

Walter M. Osborn and Roy D. Hager

Lewis Research Center
Cleveland, Ohio 44135

NATIONAL AERONAUTICS AND SPACE ADMINISTRATION • WASHINGTON, D. C. • JANUARY 1976

1. Report No. NASA TN D-8131	2. Government Accession No.	3. Recipient's Catalog No.
4. Title and Subtitle EFFECTS OF FOUR INLET AND OUTLET TIP-ANNULUS-AREA BLOCKAGE CONFIGURATIONS ON THE PERFORMANCE OF AN AXIAL-FLOW FAN ROTOR		5. Report Date January 1976
		6. Performing Organization Code
7. Author(s) Walter M. Osborn and Roy D. Hager		8. Performing Organization Report No. E-8466
		10. Work Unit No. 505-04
9. Performing Organization Name and Address Lewis Research Center National Aeronautics and Space Administration Cleveland, Ohio 44135		11. Contract or Grant No.
		13. Type of Report and Period Covered Technical Note
12. Sponsoring Agency Name and Address National Aeronautics and Space Administration Washington, D. C. 20546		14. Sponsoring Agency Code

15. Supplementary Notes

16. Abstract

An axial-flow fan rotor was tested with four configurations of tip-annulus-area blockage to speeds as high as 0.8 of design speed. The rotor performance with the four blockage configurations is compared with the unblocked rotor performance and with blockage configurations previously investigated. The blockage configurations enable the rotor to operate in a stable condition, to much lower flows than the unblocked rotor, with no evidence of rotating stall. The blockage configurations were effective in reducing rotor torque and weight flow but were accompanied by reductions in pressure ratio and efficiency.

17. Key Words (Suggested by Author(s)) Compressors; Flow blockage; Torque reduction; Rotating stall	18. Distribution Statement Unclassified - unlimited STAR Category 02 (rev.)

19. Security Classif. (of this report) Unclassified	20. Security Classif. (of this page) Unclassified	21. No. of Pages 26	22. Price* $3.75

* For sale by the National Technical Information Service, Springfield, Virginia 22161

EFFECTS OF FOUR INLET AND OUTLET TIP-ANNULUS-AREA BLOCKAGE CONFIGURATIONS ON THE PERFORMANCE OF AN AXIAL-FLOW FAN ROTOR

by Walter M. Osborn and Roy D. Hager

Lewis Research Center

SUMMARY

An axial-flow fan rotor was tested with four tip-annulus-area blockage configurations to speeds as high as 0.8 of design speed. All of the blockage configurations suppressed rotating stall and enabled the rotor to operate in a stable condition to much lower flows than the unblocked rotor. The investigation indicated that a blockage device might be applicable for reducing fan rotor torque to ease engine starting requirements and also for reducing weight flow to control engine thrust.

Blockage configurations tested in the present investigation were compared with outlet annulus-area blockage configurations previously investigated. The outlet blockage configuration appears to be a good choice for a blockage device from the overall viewpoint of performance, ease of installation, and safety aspects (outlet blockage). The torque reductions obtained with the outlet configuration were not as great as for the other two basic configurations but may be adequate for reducing starting fan torque. Where torque reduction is the main consideration, the contoured inlet-outlet blockage configuration should be considered. The reductions of pressure ratio and efficiency were greatest with the contoured inlet blockage configuration, which may limit its usefulness.

At low-flow-rate conditions, temperature measurements indicated the presence of backflows or eddy flows at both the rotor inlet and outlet for all of the blockage configurations tested. At the maximum-efficiency point, the eddy flows at the rotor inlet disappeared for all of the blockage configurations, but rotor-outlet eddy flow persisted for two of the blockage configurations.

INTRODUCTION

The turbofan engine, with its division of inlet air into bypass air and core engine air, is well suited for the application of a flow blockage device in the fan bypass air duct. Such a blockage device may be used for reducing the engine starting torque requirements, for delaying or suppressing rotating stall in order to reduce inlet-stage rotor blade stress, for thrust control, and possibly for improving the acceleration characteristics of some engines.

Three fan bypass ratios were simulated in the investigation of reference 1 by inserting different tip-annulus-area blockage rings downstream of a fan-type rotor. In reference 2, two door positions of a blockage device were also simulated by using blockage rings. All of these blockage configurations lowered the rotor torque requirements, suppressed rotating stall, and maintained stable rotor operating conditions at much lower flow rates than was possible with the unblocked rotor.

In the investigation of a 13-stage axial-flow compressor (ref. 3), inlet tip baffles (blockage) successfully suppressed rotating stall and reduced blade vibratory stress in the inlet-stage rotor. However, in the investigation of a 15-stage compressor (ref. 4), inlet tip baffles were not effective in reducing blade stresses. Thus, experimental testing appears to be required for each compressor design in order to determine the effectiveness of various blockage techniques.

This investigation was conducted to further determine the effectiveness of several annulus-area blockage configurations in the suppression of rotating stall and to evaluate the effect of the blockage upon rotor torque, pressure ratio, efficiency, and weight flow. The rotor performances obtained with the blockage configurations used in this report and in reference 1 are compared. The annulus-area blockages were chosen to give nominal area blockages of 22 and 55 percent.

SYMBOLS

C contoured blockage

F front blockage

N rotative speed, rpm

N_D equivalent design speed, $N/\sqrt{\theta}$, 16 000 rpm

R rear blockage

T total temperature (corrected to standard-day conditions)

W weight flow, kg/sec (lbm/sec)

δ ratio of rotor-inlet total pressure to standard pressure of 10.13 N/cm^2 (14.69 psia)

η adiabatic temperature-rise efficiency

θ ratio of rotor-inlet total temperature to standard temperature of 288.2 K (518.7° R)

APPARATUS AND PROCEDURE

Test Facility

A schematic of the test facility is shown in figure 1. The facility is sized for a maximum flow rate of 45.4 kilograms per second (100 lbm/sec). The drive system consists of a 11 186-kilowatt (15 000-hp), 3600-rpm, electric motor with a variable-frequency speed control. The motor is coupled to a 5.02:1 ratio speed increaser gearbox that drives the test rotor. For the present study, air entered the test facility at an inlet on the roof of the building and was exhausted to a low-pressure (vacuum) exhaust system.

Test Rotor

The test rotor is shown in figure 2. The rotor had 47 blades, a nominal tip diameter of 50.8 centimeters (20 in.), and a hub-tip radius ratio of 0.5 at the inlet. The design tip diffusion factor was 0.45. The equivalent design operating speed N_D was 16 000 rpm, or an inlet tip speed of approximately 426 meters per second (1396 ft/sec). The rotor was equipped with blade vibration dampers (fig. 2). Ten blades were instumented with strain gages in order to monitor the blade stress during the investigation. A more detailed description of the test rotor and its performance is given in reference 5.

Blockage Configurations

Profiles of the blockage configurations tested are shown in figure 3. The outlet blockage rings were the same rings that were used in the investigation of reference 1. The inner radii of the outlet blockage rings were chosen to block 22 or 55 percent of the flow, based upon the design flow streamlines. The same radii were used for the inlet blockage rings. For outlet blockage, the actual annulus-area blockages at the upstream edge of the annular block (close behind the rotor) corresponding to the nominal values (22 and 55 percent) were 23.9 and 55.7 percent, respectively. For inlet blockage, the actual annulus-area blockages at the downstream edge of the annular block (just ahead of the rotor) corresponding to the nominal values were 24.6 and 49.5 percent. Hereinafter the designation "area" or "flow" in front of the blockage will be dropped, and the blockage configurations will simply be referred to as blockage preceded by their nominal values. Also, the letters "F" for front and "R" for rear will be substituted for inlet and outlet, respectively, with the letter "C" indicating that the front blockage is contoured into the casing at the inlet. Thus, the blockage configuration shown in figure 3(a) is referred to as 22(CF-R). The configurations shown in figures 3(b) to (d) are referred to as 55(CF-R), 55(CF), and 55(F-R), respectively.

Instrumentation

The instrumentation is nearly the same as that used in the investigation of reference 5 for determining the overall and blade-element performance of the rotor. The axial locations of the inlet and outlet survey instrumentation are shown in figure 3. At the rotor outlet, two combination probes (ref. 6) were used to measure total pressure, total temperature, and flow angle. Static pressure was measured by two $7\frac{1}{2}^{\circ}$ wedge probes. At the rotor inlet, one wedge probe and one combination probe were used. One inner-wall and one outer-wall static pressure tap were located at each of the survey planes. A hot-film probe was located at the inlet survey plane for use in determining stall.

Strain-gage-type transducers were used in measuring pressures. Iron-constantan thermocouples were used in conjunction with a constant-temperature oven to determine temperature. Flow through the compressor was determined from a thin-plate orifice. Rotor speed was measured by using a magnetic pickup in conjunction with a gear mounted on the drive-motor shaft. All data were processed by an automatic digital potentiometer and recorded on paper tape.

Test Procedure

In all tests atmospheric air entered at the rotor inlet, with the inlet flow control valve in the fully open position throughout the tests. Vacuum exhaust was used at the rotor outlet to help overcome the system losses.

For the unblocked rotor (ref. 5), test data were taken over a range of weight flows from maximum flow to stall conditions. For each weight flow, measurements were recorded at 11 radial positions. The data were obtained at 40, 50, 60, 70, 80, 90, and 100 percent of equivalent design speed. The stall points were established by increasing the backpressure (by closing the outlet flow-control valve) on the test rotor until a rapid fluctuation was noted in the signal from a hot-film probe located at the rotor inlet. Also fluctuations in compressor discharge pressure and blade stress were observed when stall was encountered. When the stalled conditions were noted, the discharge throttle was immediately opened. The weight flow was then set to within 0.5 kilogram per second (1.1 lbm/sec) of the weight flow at which stall occurred in order to obtain the performance near stall.

For the partially blocked rotor, test data were taken over a range of weight flows from the maximum flow with the outlet flow control valve fully open to the minimum flow obtainable. The minimum flow resulted from air leakage through the fully closed outlet flow-control valve. The blocked rotor was tested over a range of speeds from 0.3 to 0.7 N_D except for one configuration, which was tested to 0.8 N_D.

Performance Calculation Procedure

The data presented herein have been corrected to standard-day conditions at the plenum. The inlet flow angle was assumed to be zero degrees. The overall performance was obtained from mass-averaged survey data at the rotor-outlet and -inlet plenum values of pressure and temperature. Calculation details are given in reference 5. Inlet radial surveys of temperature and pressure were also taken 2.54 centimeters (1 in.) upstream of the blade-tip leading edge. The rotor torque was calculated from the equivalent weight flow, the rotational speed of the rotor, and the inlet plenum and outlet total temperatures.

RESULTS AND DISCUSSION

The results of this investigation are presented in three main sections: (1) rotor performance without blockage, (2) rotor performance with blockage, and (3) comparison of blocked and unblocked configurations including data obtained from reference 1.

Rotor Performance without Blockage

The rotor performance without blockage was obtained from reference 1 and is repeated herein for convenience in making comparisons with the blocked rotor performance. The unblocked rotor performance is shown in figure 4 as curves of pressure ratio, efficiency, and torque as functions of equivalent weight flow for various fractions of design speed (N_D = 16 000 rpm) from 0.4 to 1.0. At design speed, a maximum efficiency of 0.846 was obtained at a pressure ratio of 1.80 and an equivalent weight flow of 28.8 kilograms per second (63.4 lbm/sec).

Rotor performance in the stall flow regime was explored at 0.4 to 0.7 N_D. Hot-film probe surveys at the rotor inlet indicated the existence of rotating stall over the short-dashed portions of the performance curves. At the lowest weight-flow points (end points) for all of the performance curves at rotational speeds from 0.4 to 0.7 N_D, rotating stall disappeared and changed to ring stall. Rotor operation was stable at these end points, and there was a slight recovery in pressure ratio. But the efficiency was low (≈0.46).

Rotor Performance with Blockage

Rotor pressure ratio, efficiency, torque, and temperature ratio are presented as functions of equivalent weight flow for several speeds in figures 5 to 8 for blockage configurations 22(CF-R), 55(CF), 55(CF-R), and 55(F-R), respectively. In general, the performance parameters were reduced from those of the unblocked rotor, except for the ability of the blocked rotor to operate in a stable condition to much lower flows. The minimum-flow operating points for the blocked rotor were not stall limit points but resulted from flow leakage past the closed outlet flow-control valve with the facility altitude exhaust system in use. No evidence of rotating stall was detected by hot-film probe surveys at the inlet to the rotor even at the minimum-flow points. The pressure ratio at any particular speed was relatively constant over a large flow range but lessened as maximum flow was approached. The maximum efficiencies for blockages 22(CF-R) and 55(CF-R) were between 0.63 and 0.74 for the speeds investigated. The maximum efficiencies for blockage 55(CF) were lower, between 0.51 and 0.53. Only limited data were taken for blockage 55(F-R), figure 8, for comparison with blockage 55(CF-R) in order to estimate the effect of removing the contoured inlet ring. A loss of approximately 5 percentage points in maximum efficiency resulted. Low efficiencies were evidenced at the minimum-flow points even though no rotating stall patterns were indicated at the rotor inlet.

The rotor-inlet and -outlet temperature distributions for 0.7 N_D are shown in figures 9 to 11 for the minimum-flow points (parts (a)) and for the maximum-efficiency points (parts (b)) for blockage configurations 22(CF-R), 55(CF), and 55(CF-R), respectively.

For the minimum-flow points (figs. 9(a), 10(a), and 11(a)), the temperature at the rotor inlet near the blade hub was greater than standard-day temperature and increased toward the blade tip. The temperature at the rotor outlet also increased from the blade hub toward the tip for the three blockage configurations. The test results for the unblocked rotor at a similar operating point (ref. 5) indicated a constant inlet temperature at standard-day conditions and an outlet temperature that decreased slightly from the rotor hub to the tip. Thus, at the minimum-flow point it appears that reverse or eddy flows are indicated in the outer portions of the blade at both the rotor inlet and outlet for all three blockage configurations.

For the maximum-efficiency points (figs. 9(b), 10(b), and 11(b)), the inlet temperature was nearly constant and equal to standard-day conditions. The outlet temperature increased from the blade hub toward the tip for blockage configurations 22(CF-R) and 55(CF) but decreased slightly for blockage configuration 55(CF-R). The test results for the unblocked rotor at a similar operating point (ref. 5) indicated a constant inlet temperature at standard-day conditions and an outlet temperature that was approximately constant. Thus, no eddy flows are indicated at the inlet for the three blockage configurations. Eddy flows at the rotor outlet in the outer portions of the blades are indicated for the 22(CF-R) and 55(CF) blockage configurations but not for the 55(CF-R) configuration. For this configuration (fig. 11), the inner radius of the blockage was in line with the blade dampers, and any eddy flow was probably confined to the region between the blade damper and the blade tip, with little or no mixing with the main stream. This may account for the higher efficiency of this blockage configuration, and it may not be representative for rotors without blade vibration dampers or with dampers at a radius different from the inner radius of the blockage.

Comparison of Unblocked and Blocked Rotor Configurations

The performance parameters may be compared for the blockage configurations by selecting operating points for each of the configurations. The operating points to be used in this comparison section were determined by the method presented in reference 1. The maximum-efficiency point of the unblocked rotor was used as a reference point. The ratio of the flow rate at the maximum-efficiency point to the maximum flow rate was obtained for the unblocked rotor. The maximum flow rates of the various blocked configurations were multiplied by this flow ratio for the unblocked rotor to obtain each of their operating points. Data presented in this section for blockages 22(R), 55(R), and 75(R) were obtained from reference 1.

Pressure ratio, efficiency, and torque as functions of weight flow at 0.7 N_D for blockages 55(CF-R), 55(CF), and 55(R) and for the unblocked rotor are shown in figure 12. The stall limit line for the unblocked rotor is also presented in figure 12(a) and shows that the blocked rotor can operate in a stable condition to much lower flows than the unblocked rotor. The calculated operation points for the blocked configurations are shown by solid symbols, as is the maximum-efficiency reference point of the unblocked rotor. Reductions in weight flow, pressure ratio, efficiency, and torque resulted at the operating points of the blocked rotor as compared to the unblocked rotor. Similar operating points may be calculated for the other blockage configurations.

Pressure ratio, efficiency, torque, and weight flow as functions of the percentage of flow blockage at 0.7 N_D and 0.5 N_D are shown in figure 13 for all of the blockage configurations tested in both this investigation and the investigation of reference 1. The points shown are the performance of the blocked rotor at the calculated operating points referenced to the unblocked maximum-efficiency point. Curves are drawn through the operating points for only 0.7 N_D; however, the trends are similar for 0.5 N_D (solid symbols). Only for the R blockage configuration were data obtained with blockages of 22, 55, and 75 percent. A dashed estimated curve is shown for CF blockage between 0 and 55 percent of total flow as this configuration was not tested with 22 percent blockage. Also, for the CF-R configuration, the efficiency (fig. 13(b)) is shown as a dashed curve between 22 and 55 percent blockage. (The efficiency at 55 percent blockage may not be representative, as pointed out in an earlier section, because of the blade dampers being at the same radius as the inner radius of the blockage.) Curves are not drawn through the weight flow data shown in figure 13(d), but instead the data are shown in relation to a dashed line representing a 1:1 ratio (i.e., 55 percent blockage results in 55 percent reduction in weight flow). From figure 13, the effects of blockage on rotor performance may be estimated for blockages other than those used in this investigation and the investigation of reference 1.

The reductions in torque and weight flow and the losses in pressure ratio and efficiency at the calculated operating points are given in table I for all of the blockage configurations tested.

Reductions in torque of between 27 and 55 percent were obtained with the various blockage configurations except for configuration 22(R), which had a reduction of only 19 percent. Such torque reductions could be used to ease engine starting requirements. Between 0 and 55 percent blockage, the CF-R configuration gave the greatest torque reduction and the R configuration gave the least reduction.

The reductions in weight flow ranged from 15 to 72 percent for the various blockages. For the CF-R configuration, the percentage of weight flow reduction was approximately equal to the nominal percentage of blockage. The results presented in reference 2 indicated that stable rotor operation could be maintained while blockage doors were moved through an arc of 0° to 90°. Thus, the weight flow reductions that could be obtained by blocking the fan bypass air might be used as a method of controlling thrust while maintaining high engine speed. Between 0 and 55 percent blockage, the largest weight-flow reductions were obtained with the CF-R and R blockage configurations (about equal); the CF blockage configuration gave the least reduction.

The reductions in pressure ratio associated with the various blockage configurations were between 5 and 15 percent. The R configuration gave the smallest reduction; and the CF configuration, the greatest reduction.

The reductions in efficiency due to the blockages were between 21 and 52 percentage points, with the CF configuration giving the greatest loss. The lowest efficiency loss (21 points) was obtained with the 55(CF-R) configuration. However, this low loss could well be the result of the blade dampers being in line with the blockage contours and may not be representative for other rotors.

CONCLUDING REMARKS

The design tip speed for the rotor used in this investigation was approximately 426 meters per second (1396 ft/sec). At 0.7 N_D, the tip speed was 298 meters per second (977 ft/sec), at which speed the unblocked rotor peak efficiency was 0.896 with a pressure ratio of 1.306. Thus, the blockage data presented in this investigation and the investigations of references 1 and 2 for 0.7 N_D and lower may be applicable to many present-day fan engines.

The blockage configurations tested in this investigation and in the investigations of references 1 and 2 suppressed rotating stall at rotor speeds as high as 0.7 N_D. The suppression of rotating stall resulted in low blade vibratory stresses and enabled the rotor to operate in a stable condition to very low flows. At low flow conditions, eddy flows or backflows occurred near the rotor tip for all of the blockage configurations. The eddy might have the appearance of ring stall encompassing the rotor tip. It was sufficiently axially symmetric that unsteady conditions were not imposed on the blade forces, as is usually noted when rotating stall is present. Apparently, this ring stall was stable. Its size increased as the rotor backpressure and blockage were increased, and rotating stall did not occur.

The losses incurred in the eddy were reflected in losses in overall efficiency and in an increase in temperature near the blade-tip region. It may be necessary to limit the operating time with high percentages of blockage, especially at high rotational speeds, because of this increase in temperature in the rotor tip region. One way to alleviate the high-temperature condition and still maintain stable operation would be to allow a small air leakage through the blocked region.

It appears that a device for partially blocking the fan bypass airflow is feasible (ref. 2). Such a blockage device could be used to obtain several beneficial modes of engine operation: (1) greater flexibility in operation as a result of the wide range of stable flow and pressure conditions made available with partial flow blockage, (2) reduced engine starting torque requirements and thus the use of lower-cost starting components, and (3) reduced thrust at high engine rotational speed for maneuvers in which quick thrust recovery would be an advantage and could be obtained by rapidly opening the blockage doors.

The choice of a blockage configuration to obtain these benefits may be influenced by factors other than performance, such as the ease of installation and safety aspects. Rear blockage would be the best choice for a blockage configuration, considering these aspects. From the standpoint of performance, the rear blockage configuration as compared with the other two configurations (CF-R and CF) is good for maintaining pressure ratio and efficiency and for reducing weight flow. Its torque reduction is not as large as that obtained with the other two configurations. However, reductions of 34 percent with 55 percent blockage and 49 percent with 75 percent blockage may be adequate for reducing starting torque requirements. Thus, it appears that the rear blockage configuration would be the best overall choice for a blockage device.

If torque reduction is the prime consideration, the CF-R configuration should be considered. This configuration is also good for reducing weight flow and maintaining pressure ratio and efficiency. But it requires a more complicated installation than the other two configurations. The CF configuration appears to be the least desirable configuration as it has the largest reduction of pressure ratio and efficiency. Both the CF-R and CF blockage configurations also have a potential safety hazard in that blockage is located upstream of the fan.

The stable rotor operation at low flows obtained with the 22(CF-R) blockage configuration suggests the possibility of using the CF-R configuration with a very low percentage of blockage (<5 percent) so that the rotor tip would be operating in a shallow groove. Such blockage, in this case perhaps more appropriately called "rotor tip treatment," might result in increased flow range and stall margin with little loss in overall performance.

SUMMARY OF RESULTS

An inlet-stage, axial-flow fan rotor was tested with tip-annulus-area blockage to speeds as high as 0.8 of design speed. The blockage data obtained may be applicable to many present-day fan engines. At 0.7 of design speed (298 m/sec (977 ft/sec) tip speed), the peak efficiency of the unblocked test rotor was 0.896 with a pressure ratio of 1.306.

Four blockage configurations were tested: one with 22 percent and three with 55 percent blockage. The blockages suppressed rotating stall and enabled the rotor to be operated in a stable condition to much lower flows than the unblocked rotor. The investigation indicated that a blockage device might be applicable for reducing fan torque to ease engine starting requirements and for reducing weight flow to control engine thrust.

The following results were obtained with blockage, at 0.7 of design speed:

1. Based on calculated operating points referenced to the unblocked rotor's maximum-efficiency point, blockage configuration 22(CF-R) resulted in reductions in torque (41 percent), weight flow (22 percent), pressure ratio (11 percent), and efficiency (30 percentage points). Corresponding reductions for the 55(CF-R) blockage configuration are 55, 54, 5, and 21. Similarly, blockage configuration 55(CF) gave reductions of 42, 45, 14, and 52.

2. The maximum efficiency obtained with a blunt upstream blockage configuration (55(F-R)) was 5 percentage points lower than that obtained when the upstream blockage was contoured into the outer casing (55(CF-R)).

3. At low flow rates, eddy flows or backflows are indicated at both the rotor inlet and outlet for all of the blockage configurations. At the maximum-efficiency point, the eddy flows at the inlet disappeared for all of the blockage configurations. Eddy flow at the outlet disappeared for the 55(CF-R) blockage configuration but not for the 22(CF-R) and 55(CF) blockage configurations.

Lewis Research Center,
National Aeronautics and Space Administration,
Cleveland, Ohio, October 1, 1975,
505-04.

REFERENCES

1. Osborn, Walter M.; and Lewis, George W., Jr.: Effects of Three Outlet-Annulus Area Blockage Configurations on the Performance of a 20-Inch (50.8 cm) Axial-Flow Compressor Rotor. NASA TN D-5506, 1969.
2. Osborn, Walter M.; and Wagner, Jack M.: Effect of Simulated Downstream Flow Blockage Doors on the Performance of an Axial-Flow Fan Rotor. NASA TN D-6071, 1970.
3. Huntley, Sidney C.; Huppert, Merle C.; and Calvert, Howard F.: Effect of Inlet-Air Baffles on Rotating-Stall and Stress Characteristics of an Axial-Flow Compressor in a Turbojet Engine. NACA RM E54G09, 1955.
4. Lucas, James G.; Finger, Harold B.; and Filippi, Richard E.: Effect of Inlet-Annulus Area Blockage on Over-All Performance and Stall Characteristics of an Experimental 15-Stage Axial-Flow Compressor. NACA RM E53L28, 1954.
5. Hager, Roy D.; Janetzke, David C.; and Reid, Lonnie: Performance of a 1380-Foot-Per-Second-Tip-Speed Axial-Flow Compressor Rotor with a Blade Tip Solidity of 1.3. NASA TM X-2448, 1972.
6. Glawe, George E.; Krause, Lloyd N.; and Dudzinski, Thomas J.: A Small Combination Sensing Probe for Measurement of Temperature, Pressure, and Flow Direction. NASA TN D-4816, 1968.

TABLE I. - EFFECT OF BLOCKAGE ON ROTOR PERFORMANCE

AT 0.7 EQUIVALENT DESIGN SPEED

[Based on calculated operating points for blocked rotor referenced to maximum-efficiency point (η = 0.896) of unblocked rotor.]

Blockage configuration	Reduction in pressure ratio, percent	Reduction in efficiency, percentage points	Reduction in weight flow, percent	Reduction in torque, percent
22(CF) estimated	15	33	15	27
22(CR-R)	11	30	22	41
22(R)	7	24	15	19
55(CF)	14	52	45	42
55(CF-R)	5	21	54	55
55(R)	5	41	56	34
75(R)	7	50	72	49

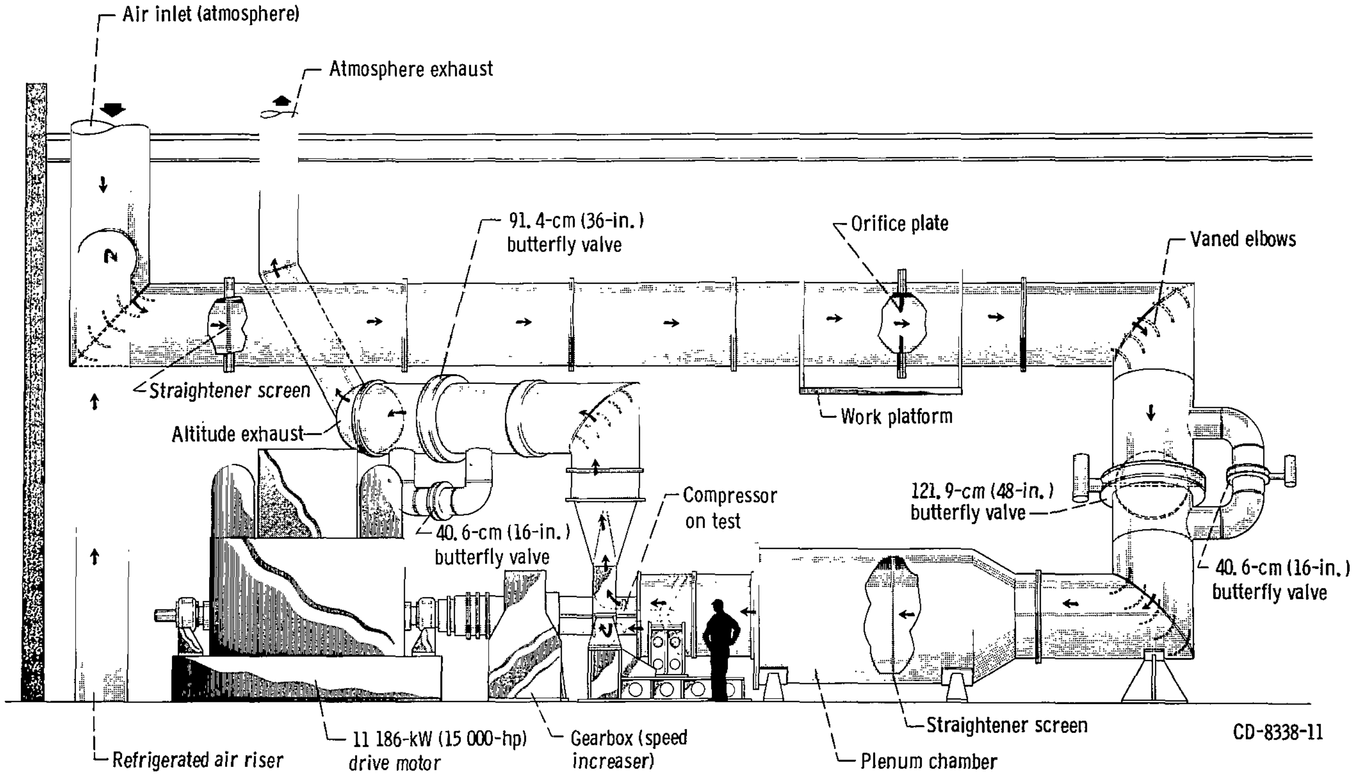

Figure 1. - Test facility.

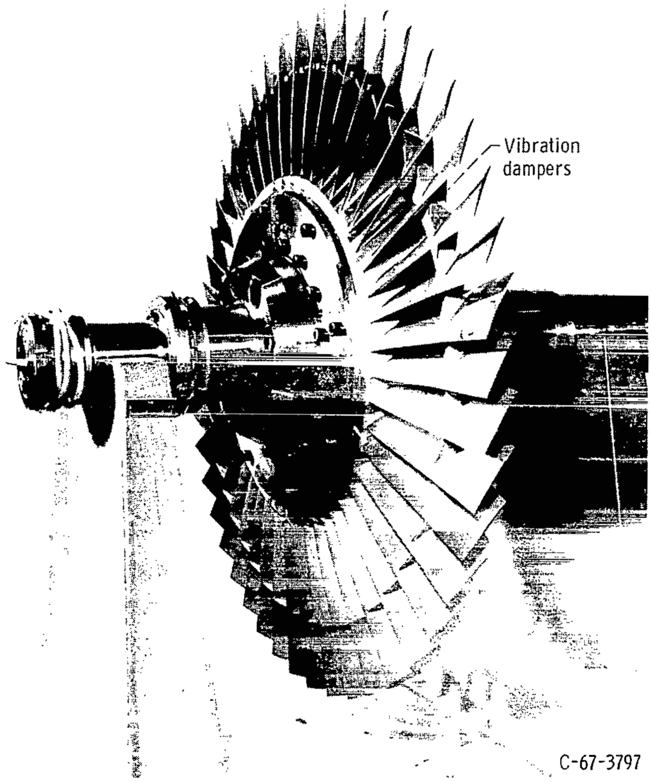

Figure 2. - 50.8-Centimeter (20-in.) axial-flow fan rotor.

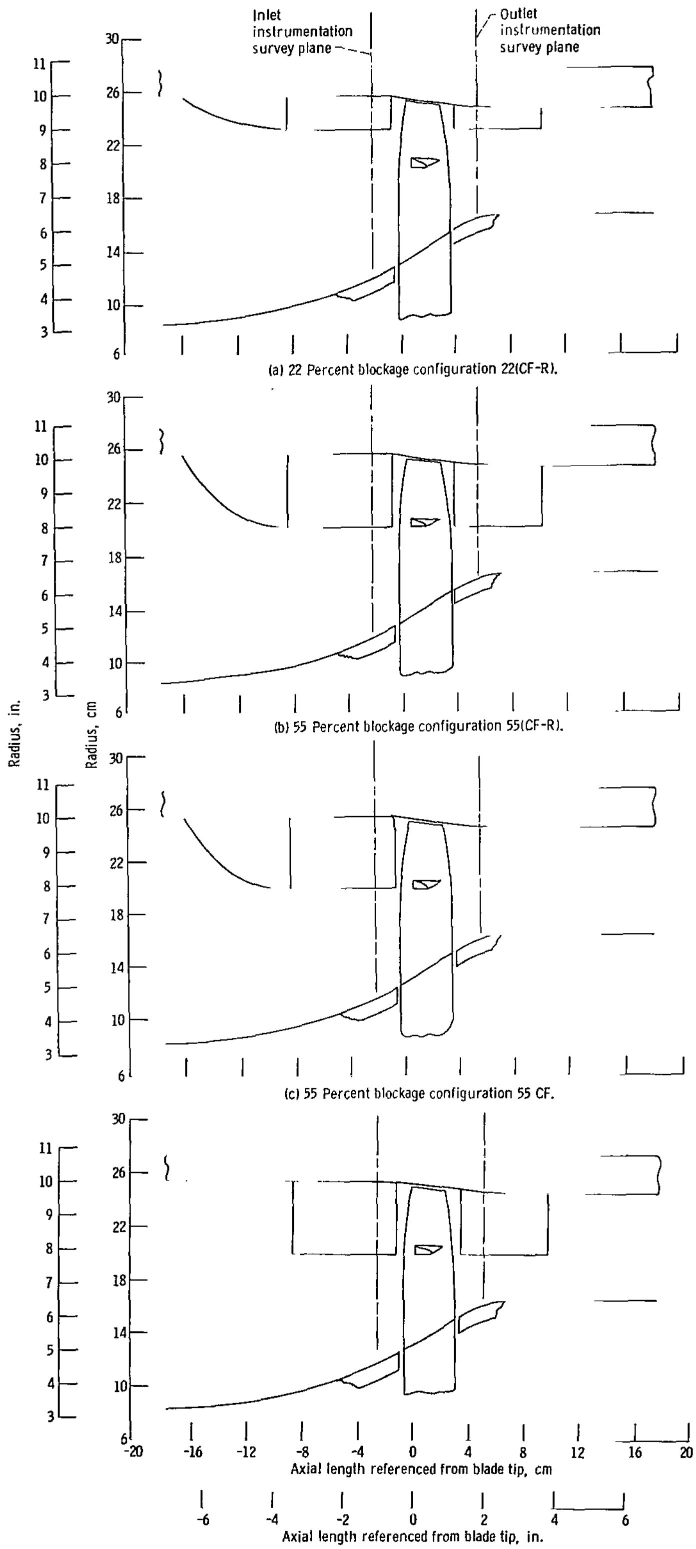

(d) 55 Percent blockage configuration 55(F-R).

Figure 3. - Meridional view of axial-flow rotor showing blockage configurations.

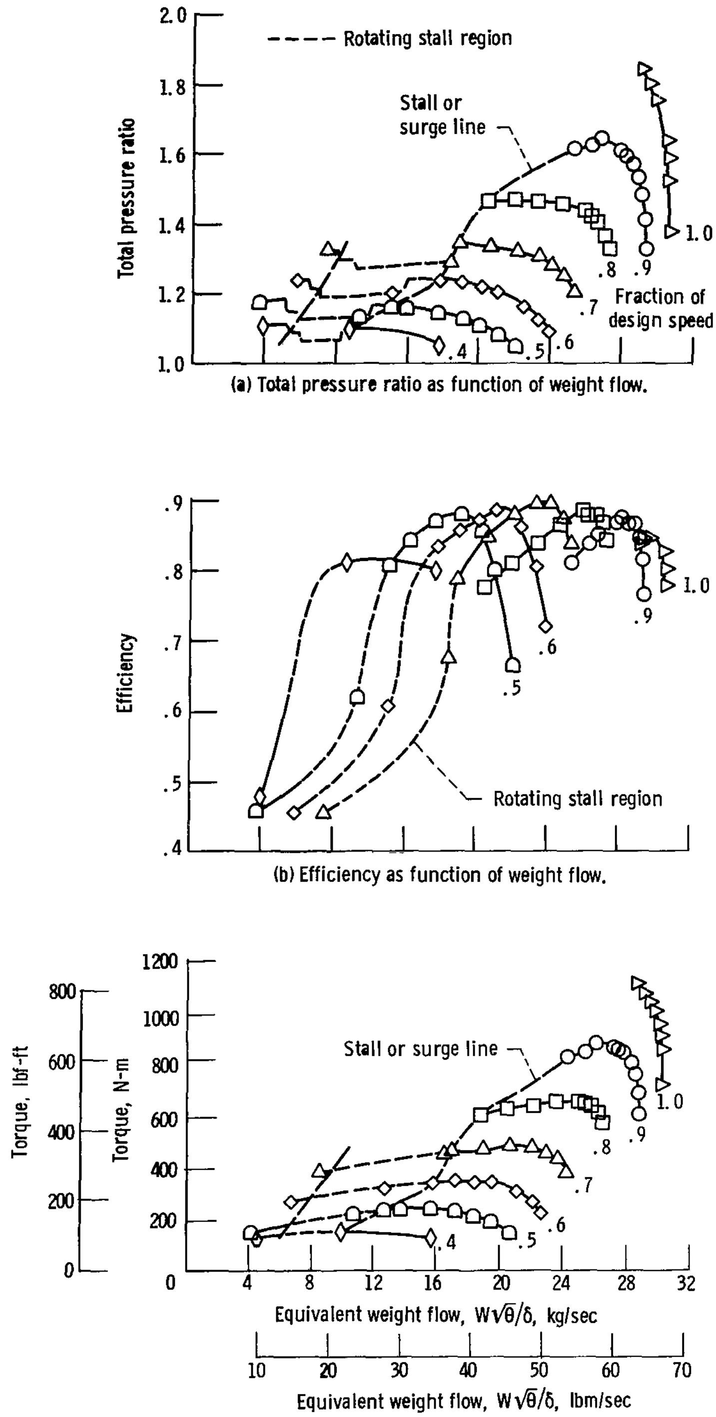

(c) Torque as function of weight flow.

Figure 4. - Rotor performance without blockage.

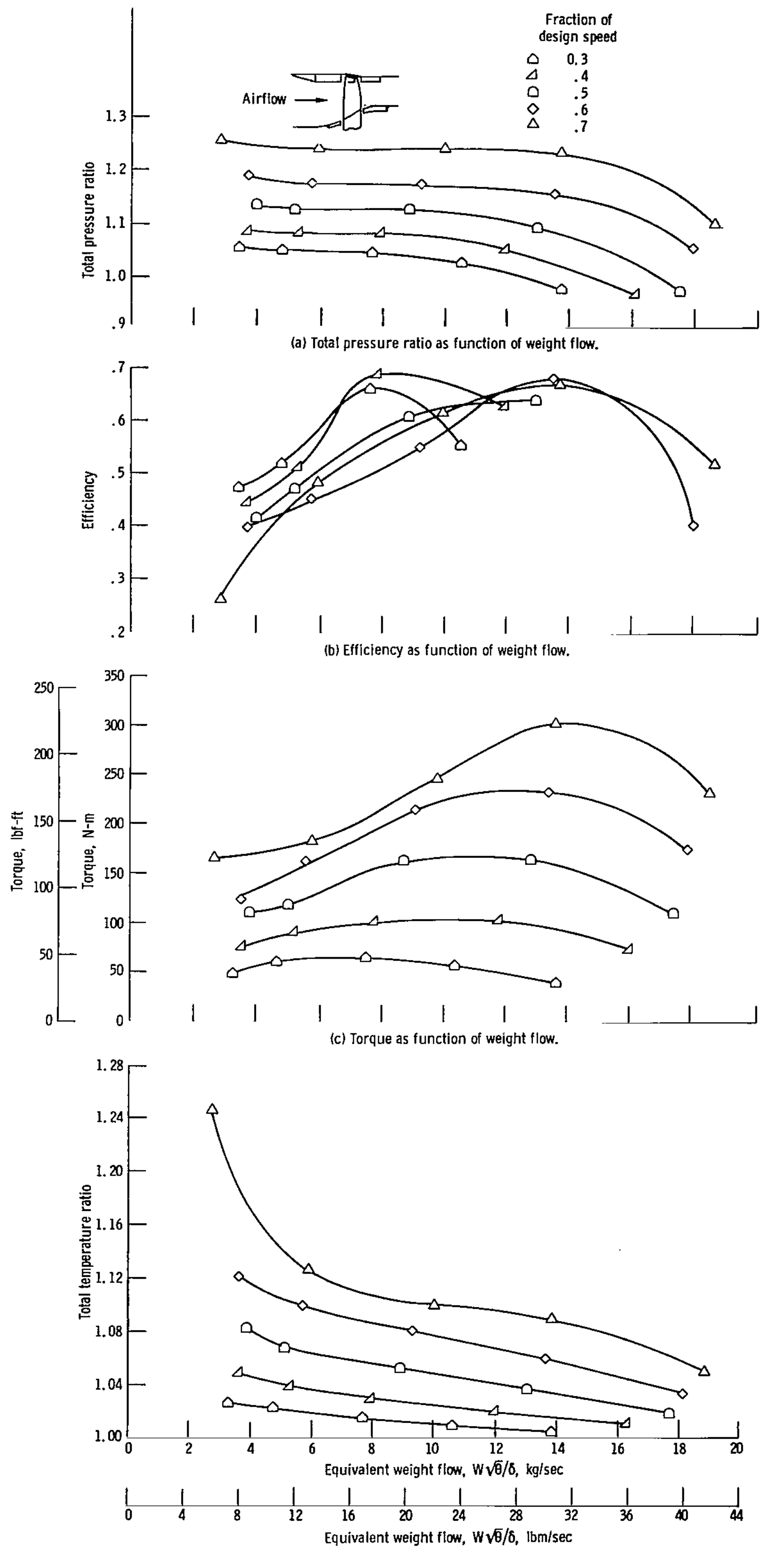

Figure 5. - Rotor performance for 22(CF-R) blockage configuration.

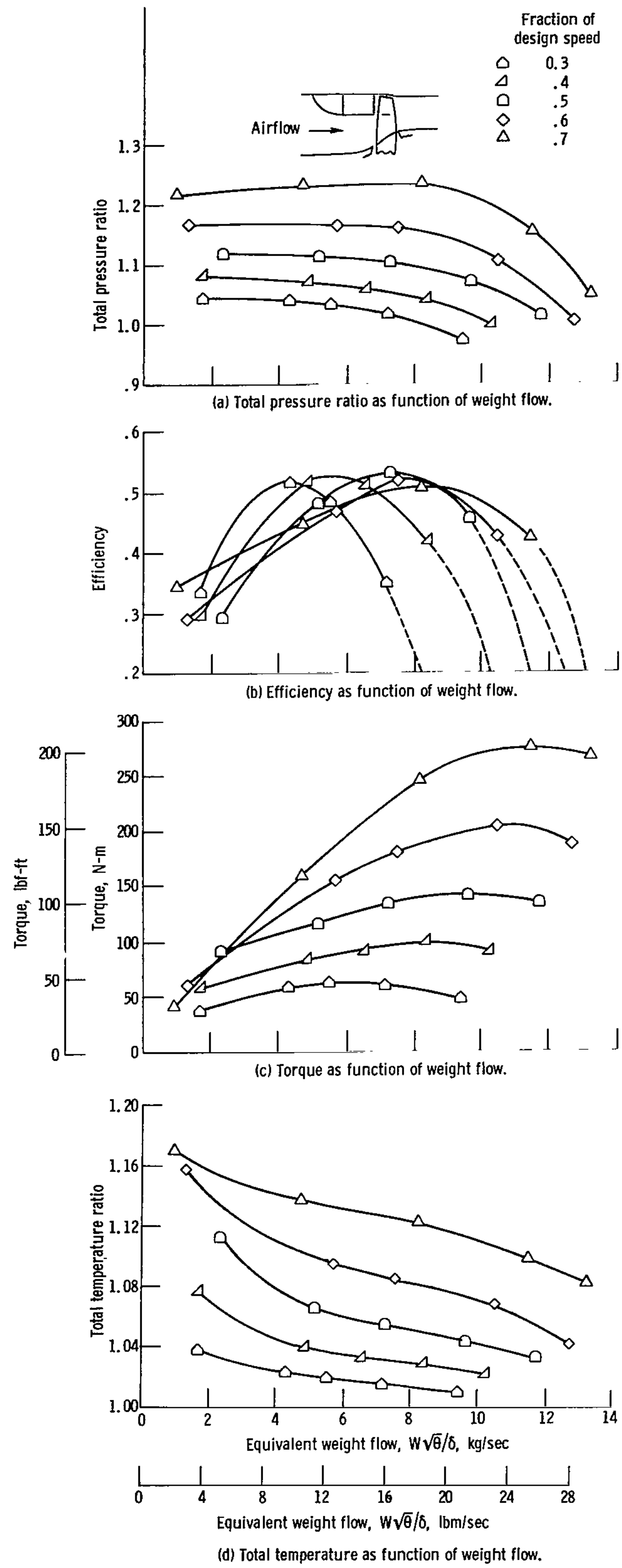

Figure 6. - Rotor performance for 55(CF) blockage configuration.

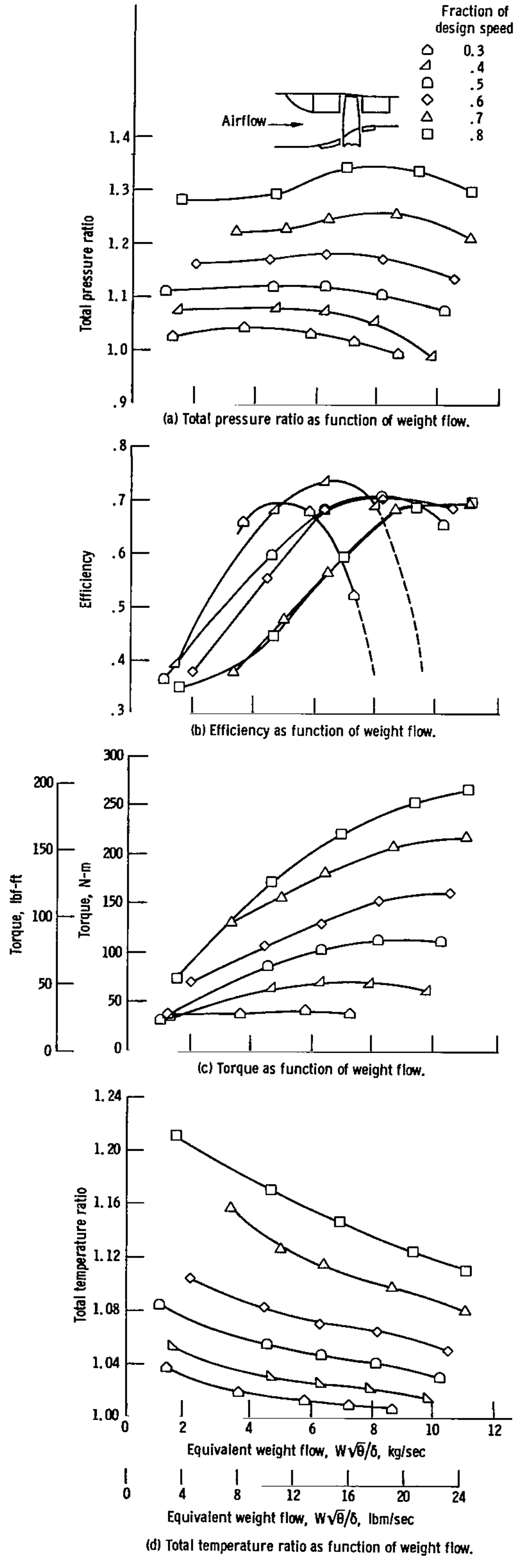

Figure 7. - Rotor performance for 55(CF-R) configuration.

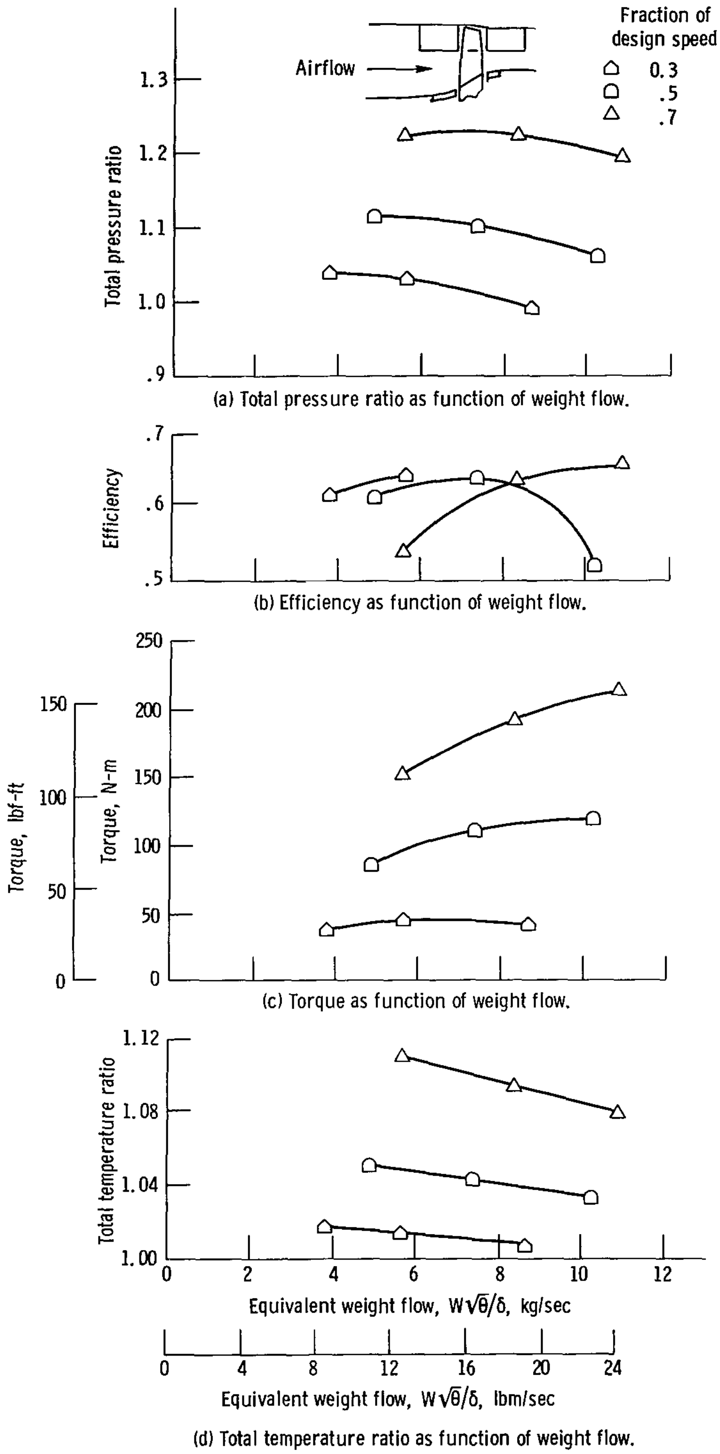

Figure 8. - Rotor performance for 55(F-R) blockage configuration.

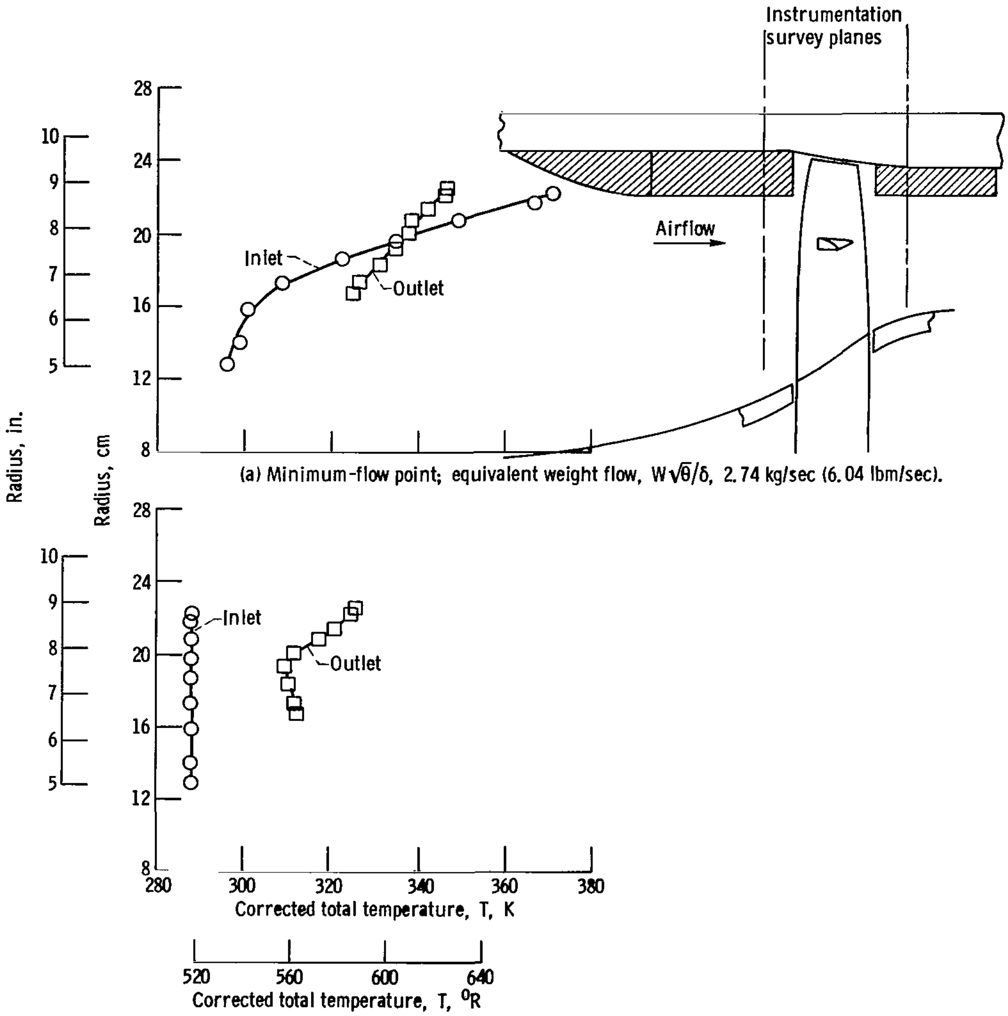

(b) Maximum-efficiency point; equivalent weight flow, $W\sqrt{\theta}/\delta$, 13.82 kg/sec (30.47 lbm/sec).

Figure 9. - Inlet and outlet total temperature profiles for rotor with 22(CF-R) blockage configuration. Speed, 0.7 of design speed.

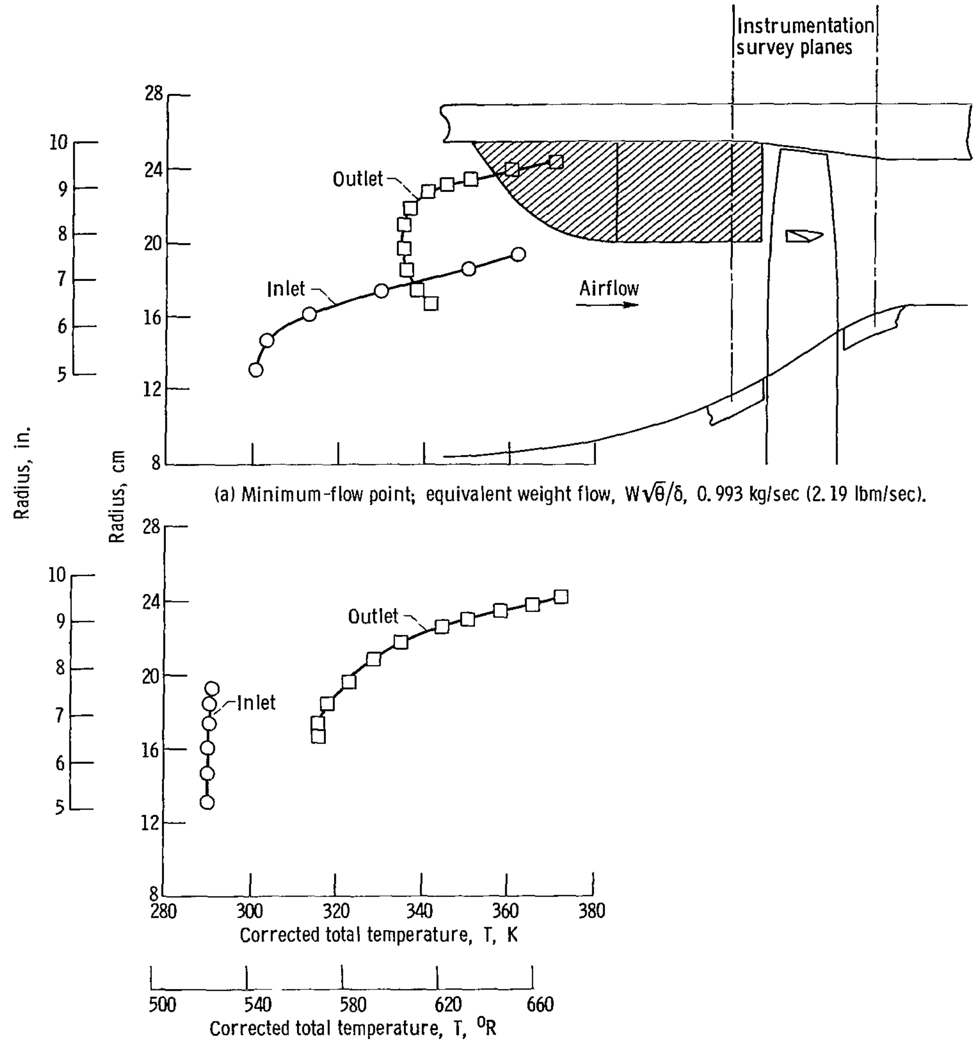

(b) Maximum-efficiency point; equivalent weight flow, $W\sqrt{\theta}/\delta$, 8.24 kg/sec (18.16 lbm/sec).

Figure 10. - Inlet and outlet total temperature profiles for rotor with 55(CF) blockage configuration. Speed, 0.7 of de$ign speed.

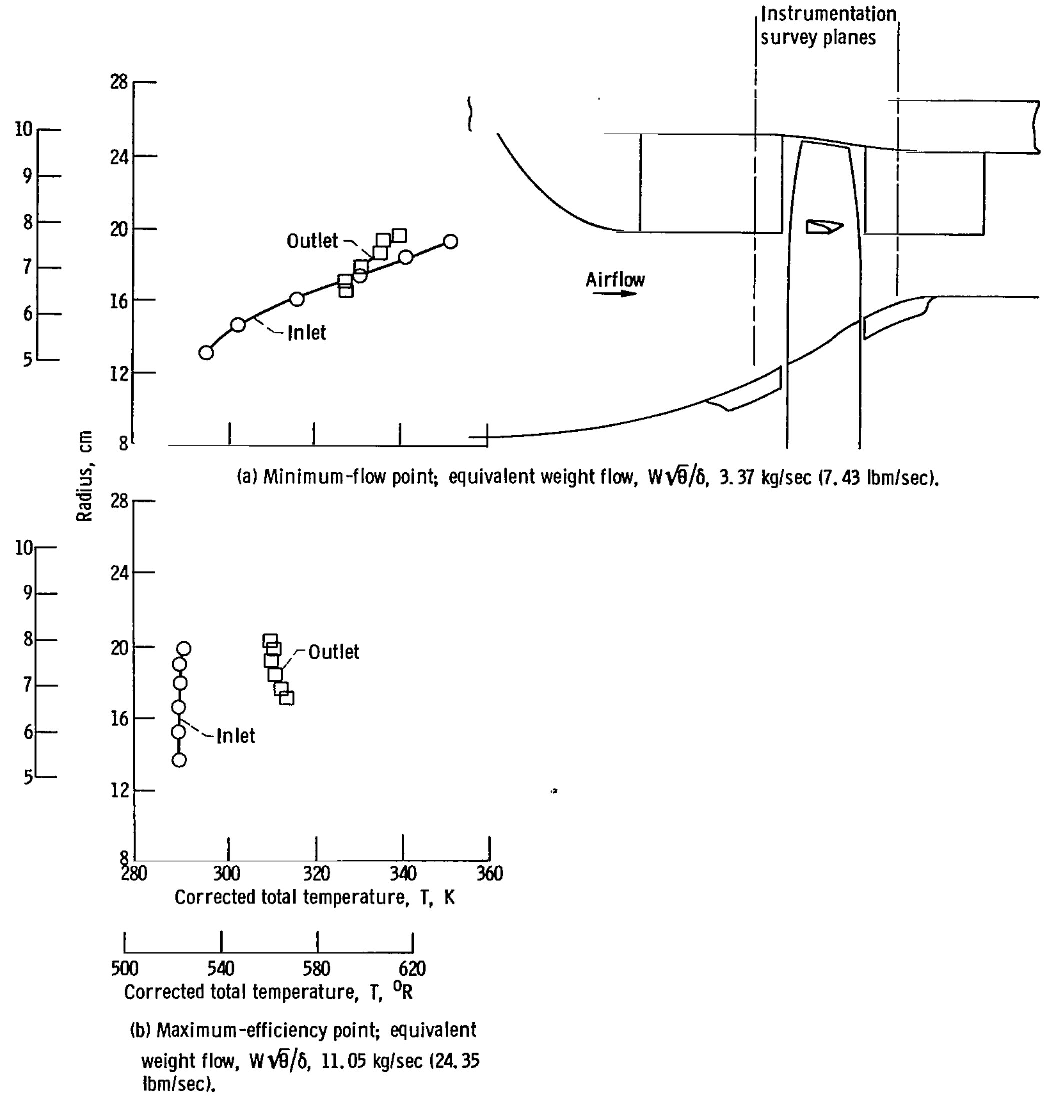

Figure 11. - Inlet and outlet total temperature profiles for rotor with 55(CF-R) blockage configuration. Speed, 0.7 of design speed.

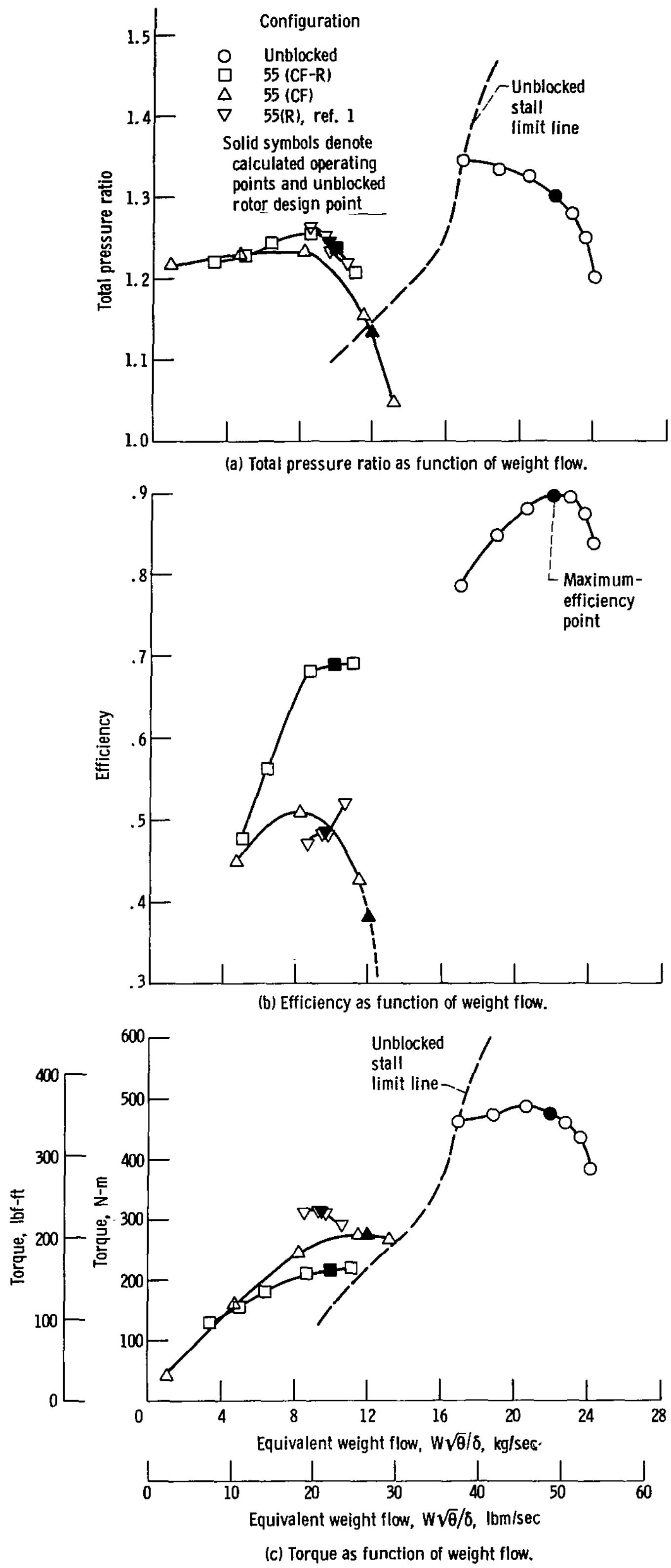

Figure 12. - Comparison of rotor performance unblocked and with 55 percent flow blockage. Equivalent speed, 0.7 of design speed.

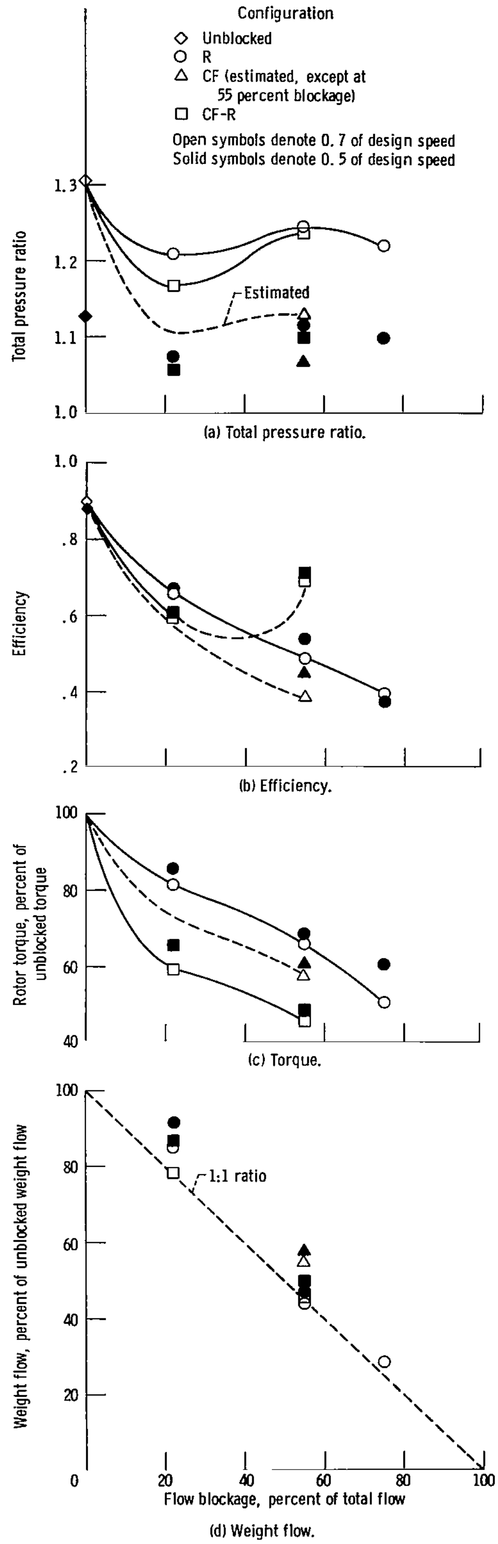

Figure 13. - Effect of several tip-annulus-area blockage configurations on rotor pressure ratio, efficiency, torque, and weight flow - referenced to unblocked maximum-efficiency point.

NATIONAL AERONAUTICS AND SPACE ADMINISTRATION
WASHINGTON, D.C. 20546

OFFICIAL BUSINESS
PENALTY FOR PRIVATE USE $300

SPECIAL FOURTH-CLASS RATE
BOOK

POSTAGE AND FEES PAID
NATIONAL AERONAUTICS AND
SPACE ADMINISTRATION
451

U.S.MAIL

189 001 C1 U A 760109 S00903DS
DEPT OF THE AIR FORCE
AF WEAPONS LABORATORY
ATTN: TECHNICAL LIBRARY (SUL)
KIRTLAND AFB NM 87117

POSTMASTER : If Undeliverable (Section 158 Postal Manual) Do Not Return

"The aeronautical and space activities of the United States shall be conducted so as to contribute . . . to the expansion of human knowledge of phenomena in the atmosphere and space. The Administration shall provide for the widest practicable and appropriate dissemination of information concerning its activities and the results thereof."

—NATIONAL AERONAUTICS AND SPACE ACT OF 1958

NASA SCIENTIFIC AND TECHNICAL PUBLICATIONS

TECHNICAL REPORTS: Scientific and technical information considered important, complete, and a lasting contribution to existing knowledge.

TECHNICAL NOTES: Information less broad in scope but nevertheless of importance as a contribution to existing knowledge.

TECHNICAL MEMORANDUMS: Information receiving limited distribution because of preliminary data, security classification, or other reasons. Also includes conference proceedings with either limited or unlimited distribution.

CONTRACTOR REPORTS: Scientific and technical information generated under a NASA contract or grant and considered an important contribution to existing knowledge.

TECHNICAL TRANSLATIONS: Information published in a foreign language considered to merit NASA distribution in English.

SPECIAL PUBLICATIONS: Information derived from or of value to NASA activities. Publications include final reports of major projects, monographs, data compilations, handbooks, sourcebooks, and special bibliographies.

TECHNOLOGY UTILIZATION PUBLICATIONS: Information on technology used by NASA that may be of particular interest in commercial and other non-aerospace applications. Publications include Tech Briefs, Technology Utilization Reports and Technology Surveys.

Details on the availability of these publications may be obtained from:

SCIENTIFIC AND TECHNICAL INFORMATION OFFICE

NATIONAL AERONAUTICS AND SPACE ADMINISTRATION

Washington, D.C. 20546